Temporal Evolution of Three-Dimensional Vortex Breakdown from Steady, Axisymmetric Solutions

Jeffrey C. Tromp* and Philip S. Beran†
U.S. Air Force Institute of Technology, Wright–Patterson Air Force Base, Ohio 45433-7521

Introduction

THE emergence and consequences of asymmetries in swirling flows that are initially steady and axisymmetric are examined. The strength of an isolated vortex in a tube is increased in a parametric fashion through a critical value, where stability to three-dimensional disturbances is lost. The flow behavior undergoes a bifurcation at the critical value from steady and axisymmetric flow to unsteady and three-dimensional flow. Other computations of bifurcation phenomena in swirling flows have been presented by Leibovich and Kribus,[1] Beran and Culick,[2] and Lopez.[3] These works are limited to bifurcations that only involve axisymmetric flows.

Axisymmetric base flows serve as initial conditions to a three-dimensional time-integration algorithm. The minimum axial velocity component $Q(t)$ is computed and compared with the initial value. Of particular interest is the characterization of the stability loss and the relationship between the appearance of asymmetries and the associated changes in Q.

The computational approach is as follows. First, a pseudo-arclength continuation (PAC) algorithm[2] provides the steady, axisymmetric initial condition for a specified vortex strength $\mathcal{V}$. The Mach number M and Reynolds number Re (based on vortex core radius) are held fixed at 0.3 and 2.5×10^2, respectively. No nonunique axisymmetric solutions are found at $Re = 2.5 \times 10^2$, consistent with Ref. 2. The two-dimensional solution is then interpolated onto the three-dimensional mesh using a fourth-order-accurate cubic spline scheme.[4] Then time integration is carried out by the time-accurate Navier–Stokes (TANS) model. The TANS model is a special-purpose, time-integration algorithm developed specifically for this work and is described in Ref. 5. The TANS model employs fourth-order compact, or Padé, operators[6] to discretize spatial derivatives, thus allowing for fewer grid nodes while maintaining sufficient accuracy. A multiblock grid is used to allow for a nearly rectilinear arrangement of nodes near the tube centerline, while near orthogonality is maintained at the tube wall. The PAC algorithm is implemented with the same boundary conditions and tube geometry as the TANS model, using a simple algebraic grid.

The physical domain consists of a two-stage cylindrical tube of circular cross section and varying radius.[2] The first stage contains a constriction that controls the upstream movement of the breakdown region. The tube radius (nondimensionalized by vortex core radius) at the inlet station is fixed at $R_0 = 2$. The number of nodes in the computational coordinate directions are (nx, ny, nz), where nx defines streamwise spacing and ny and nz are equal and define cross-plane spacing in the y and z directions, respectively. Three grids are employed in this work. Grid G1 consists of 98×41^2 nodes, grid G2 contains 122×61^2 nodes, and grid G3 uses 146×41^2 nodes. The nondimensional tube length L for grids G1 and G2 is 20, whereas the tube length for grid G3 is 30. Grid G2 uses axial clustering in the breakdown region to achieve a minimum axial spacing of about 0.1 at $x = 5$. The time step Δt for runs using grids G1 and G3 is 0.04, whereas runs on the finer grid G2 have a time step of 0.025.

Axisymmetric, columnar conditions are specified at the inflow boundary plane. The inlet axial velocity is chosen to be uniform. The swirl velocity component $\hat{v}$ is modeled from a Burger vortex and is appropriate for modeling the profiles obtained from a swirl-vane apparatus[7]:

$$\hat{v}(0, r, \theta) = \mathcal{V} r^{-1}\left(1 - e^{-r^2}\right) \tag{1}$$

where r and θ denote the radial and azimuthal coordinate directions and $\mathcal{V}$ is the vortex strength. A nonuniform inflow density profile based on columnar flow is prescribed as a Dirichlet condition.[5] Slip is allowed along the tube wall surface, yielding an impermeability boundary condition that relates the axial and radial velocities. Outflow conditions reflect an assumed columnar flow state.

Results

Between $\mathcal{V} = 1.0$ and 1.5, the initially steady, two-dimensional flow does not evolve in time to an asymmetric flow state. However, as $\mathcal{V}$ is increased slightly to 1.53, the flow becomes three dimensional and time periodic. As $\mathcal{V}$ is further increased, the magnitude of the asymmetry also increases. This change in stability is attributed to the crossing of a supercritical Hopf bifurcation point somewhere between $\mathcal{V} = 1.5$ and 1.53.

The deviations from the two-dimensional initial conditions are illustrated in Fig. 1, where Q (solid lines of Figs. 1a–1d) is plotted vs time for $\mathcal{V} = 1.5$, 1.53, 1.55, and 1.65. In Fig. 1a ($\mathcal{V} = 1.5$), it is evident that no appreciable deviation from the initial condition is present. This is confirmed by monitoring the maximum solution correction at each iteration. At $\mathcal{V} = 1.53$ (Fig. 1b), the solution departs from the initial condition, as evident by the increase in Q as time increases. The term $Q(t)$ eventually becomes time periodic, but this behavior is not discernible from the scales of the figure. Periodicity is confirmed using phase plots of the three velocity components at a fixed centerline node near $x = 7$. At $\mathcal{V} = 1.55$ and 1.65 (Figs. 1c and 1d), much larger deviations are evident.

The effect of grid resolution, time step, and tube length are also illustrated in Fig. 1. Figures 1a–1c show how grid refinement from G1 to G2 affects Q. At $\mathcal{V} = 1.5$, resolving the grid from G1 to G2 results in a slight decrease in the time-asymptotic value of Q. However, the flow remains steady and axisymmetric. At $\mathcal{V} = 1.53$, grid refinement results in a more pronounced transient response,

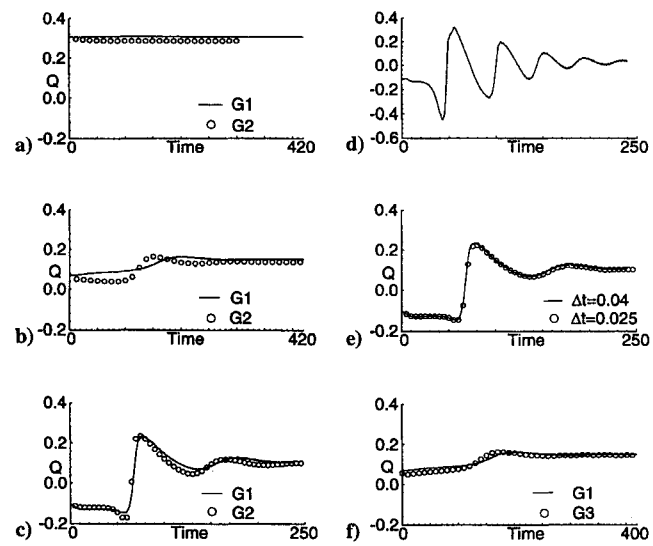

Fig. 1 Temporal behavior of Q, grid and time-step sensitivity and tube length L sensitivity: a) $\mathcal{V} = 1.5$ (G1: coarse grid, G2: fine grid, $L = 20$), b) $\mathcal{V} = 1.53$, c) $\mathcal{V} = 1.55$, d) $\mathcal{V} = 1.65$, e) effect of time step for $\mathcal{V} = 1.55$, and f) effect of tube length for $\mathcal{V} = 1.53$ (G3: coarse grid, $L = 30$).

Received Jan. 31, 1995; revision received May 16, 1995; presented as Paper 95-2310 at the AIAA 26th Fluid Dynamics Conference, San Diego, CA, June 19–22, 1995; accepted for publication Nov. 14, 1995. This paper is declared a work of the U.S. Government and is not subject to copyright protection in the United States.

*Graduate Student, Department of Aeronautics and Astronautics; currently Research Aerospace Engineer, Flight Control Division, U.S. Air Force Wright Laboratory, 2210 Eighth Street, Suite 11. Member AIAA.

†Associate Professor, Department of Aeronautics and Astronautics. Member AIAA.

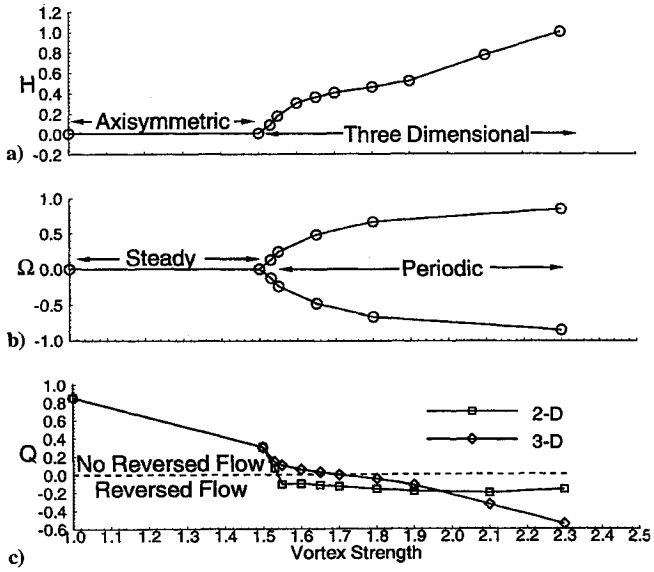

Fig. 2 Evidence of a supercritical Hopf bifurcation.

possibly representing a slight shift of the Hopf point to smaller values of vortex strength. The sensitivity to grid refinement appears to diminish as vortex strength is increased away from the Hopf point, as evident in Fig. 1c. Figure 1e shows that reducing the time step from 0.04 to 0.025, with grid G1, has a negligible influence on the transient behavior of Q. This suggests that the differences in Q evident in Figs. 1a–1c are due primarily to grid refinement and not to the reduction of the time step. Finally, the effect of tube length is shown in Fig. 1f, where increasing the tube length L from 20 to 30 appears to have a small but negligible effect on Q.

The nature of the Hopf bifurcation is illustrated in Fig. 2. To identify the onset of three-dimensionality, a global parameter H is constructed and is defined to be the maximum absolute value of $\mathrm{d}\hat{v}/\mathrm{d}\theta$. The term H is nonzero when the flow is asymmetric. In Fig. 2a, H abruptly departs from zero between $\mathcal{V} = 1.5$ and 1.53. Within this range of $\mathcal{V}$, fully three-dimensional solutions bifurcate from the branch of two-dimensional solutions when the two-dimensional solutions become physically unstable. Flow unsteadiness and asymmetry are characterized by another parameter Ω, which is defined as the minimum and maximum values of the sum of the cross-plane velocity components along the tube centerline. By definition, Ω is zero for an axisymmetric flow. In addition, since the cross-plane velocity components are unsteady, periodic functions (past $\mathcal{V} = 1.5$),

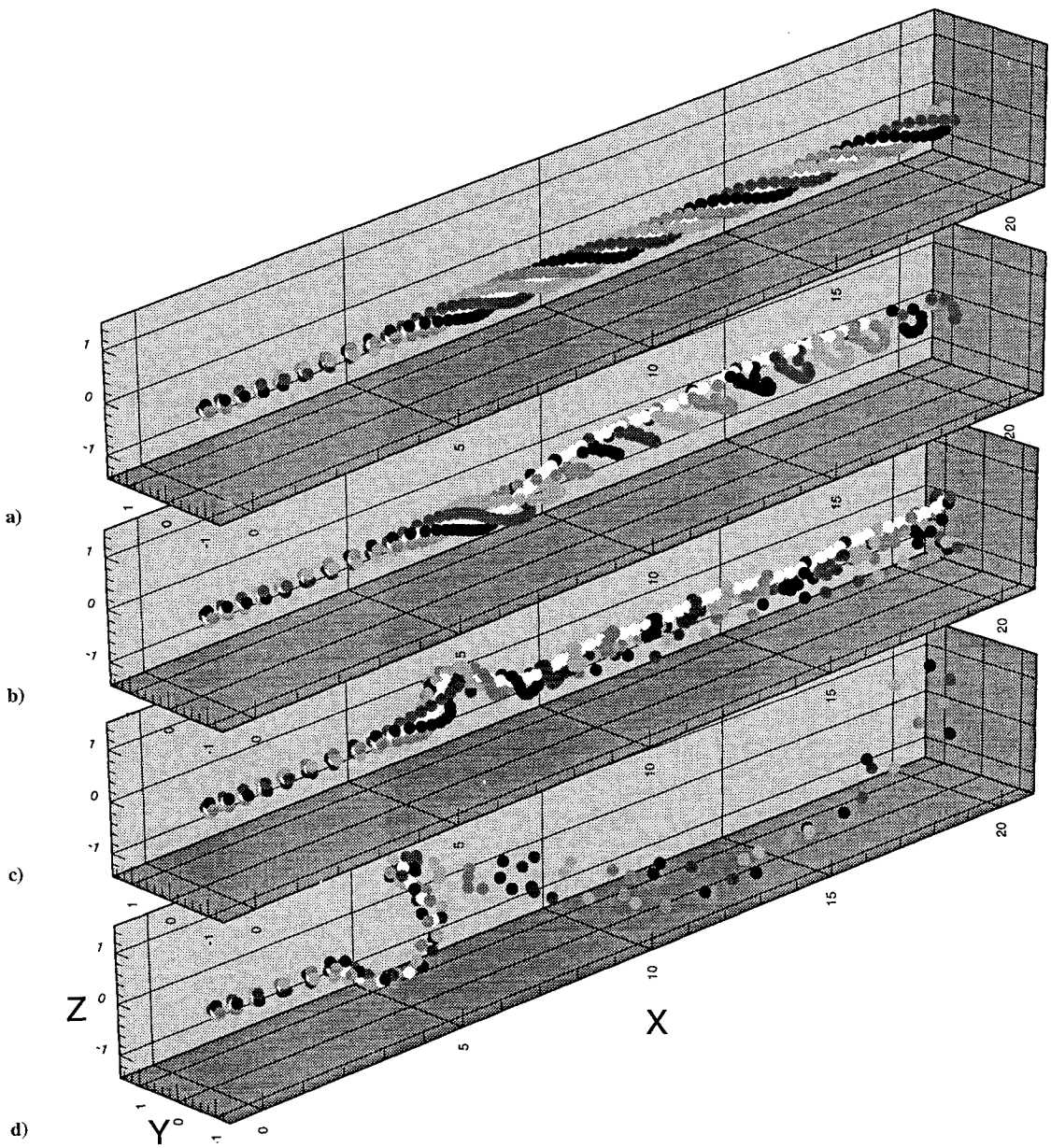

Fig. 3 Particle traces showing development of three-dimensionality with increasing vortex strength: a) $\mathcal{V} = 1.5$, b) $\mathcal{V} = 1.53$, c) $\mathcal{V} = 1.65$, and d) $\mathcal{V} = 2.3$.

Ω characterizes the degree of flow unsteadiness by representing the largest amplitude of the cross-plane velocity sum along the centerline. Figure 2b shows that Ω departs from zero at the same value of $\mathcal{V}$ that the flow becomes asymmetric. Thus, Figs. 2a and 2b demonstrate that flow unsteadiness and asymmetry are intimately linked. The loss of stability to time-periodic flow is evidence for a Hopf bifurcation. The bifurcation is supercritical,[8] since the amplitude of the disturbance, characterized by Ω, grows from zero as $\mathcal{V}$ is increased past the Hopf point. The initial and final values of Q are shown in Fig. 2c. A region in $\mathcal{V}$ exists where two-dimensional flows with bubble-type breakdown evolve into three-dimensional, unsteady flows with no reversed flow. Also, it is of interest to note that the Hopf point and the appearance of reversed flow occur at different values of $\mathcal{V}$. Thus, loss of stability is not a consequence of a gross structural change in the flowfield. Other examples in which changes in flowfield topology are disassociated from hydrodynamic bifurcations are given by Lopez.[3]

The observed increase in Q as the flow transitions from two- to three-dimensional flow is correlated to a particular asymmetric term in the governing equations. Details of this analysis can be found in Ref. 5. The correlation requires concepts put forth by Brown and Lopez[9] and Darmofal.[10] Brown and Lopez[9] established a necessary condition between the production of negative azimuthal vorticity $\hat{\eta}$ and the extent of axial flow deceleration. Consequently, the authors anticipated that the minimum azimuthal vorticity for the three-dimensional flow would be greater (less negative) than that of the initial two-dimensional flow, since Q is greater in these cases. This is indeed the case. At $\mathcal{V} = 1.5$, before the Hopf bifurcation, the minimum values of $\hat{\eta}$ computed from both the two- and three-dimensional models are virtually the same. However, just beyond the Hopf point, the minimum $\hat{\eta}$ is significantly greater in the three-dimensional flow. A numerical evaluation of asymmetric terms in the azimuthal vorticity equation is then performed.[5] This equation relates the total derivative of $\hat{\eta}$ to vorticity stretching and tilting terms.[10] Through this evaluation, it is found that the effect of three-dimensionality on radial vorticity is the principle contributor to the increase in $\hat{\eta}$. A region consisting of a positive net change in radial vorticity exists that serves to attenuate the axial deceleration process.

Flowfield visualization is performed by calculating the numerical equivalent of streaklines. Five material points are introduced into the flowfield at the inflow boundary. The white point lies initially on the tube centerline, whereas the grey scaled points lie on the y and z axes at nondimensional distances of ± 0.1 from the centerline. The material point positions are computed in time from the evolving velocity field using a first-order-accurate Euler time integration.[4] Snapshots of the time-asymptotic streaklines are shown in Fig. 3; the tube geometry is omitted for clarity. Figure 3 shows the development of three-dimensional flow as $\mathcal{V}$ is increased past the Hopf bifurcation point. At $\mathcal{V} = 2.3$ (Fig. 3d), the material points deflect off-axis in a well-defined helical-type structure, consistent with spiral-type breakdown. Further discussion of the flow visualization can be found in Ref. 5.

Conclusions

Time integration of the three-dimensional, compressible Navier–Stokes equations reveals that when the vortex strength is increased past a critical value, the time-asymptotic flow changes from axisymmetric and steady to asymmetric and time periodic, indicating a supercritical Hopf bifurcation. The three-dimensional flows form a solution branch that bifurcates from the path of two-dimensional solutions at the bifurcation point. The authors' interpretation of this result is that the mechanism for the existence of a least one family of three-dimensional solutions, which possess reversed flow at sufficiently large values of vortex strength, is the loss of stability of the axisymmetric base flows. Minimum values of axial velocity Q are observed to increase as flow asymmetries develop just beyond the Hopf point. Furthermore, a small range of $\mathcal{V}$ exists where two-dimensional solutions exhibit vortex breakdown but three-dimensional solutions do not. This attenuation of axial deceleration is found by the authors to be the result of a positive net production of radial vorticity as flow asymmetries develop.

References

[1]Leibovich, S., and Kribus, A., "Large-Amplitude Wavetrains and Solitary Waves in Vortices," *Journal of Fluid Mechanics*, Vol. 216, July 1990, pp. 459–504.

[2]Beran, P. S., and Culick, F. E. C., "The Role of Non-Uniqueness in the Development of Vortex Breakdown in Tubes," *Journal of Fluid Mechanics*, Vol. 242, Sept. 1992, pp. 491–527.

[3]Lopez, J. M., "On the Bifurcation Structure of Axisymmetric Vortex Breakdown in a Constricted Pipe," *Physics of Fluids*, Vol. 6, No. 11, 1994, pp. 3683–3693.

[4]Tromp, J. C., "The Dependence of the Time-Asymptotic Structure of 3-D Vortex Breakdown on Boundary and Initial Conditions," Ph.D. Dissertation, Dept. of Aeronautics and Astronautics, U.S. Air Force Inst. of Technology, Wright–Patterson AFB, OH, 1995.

[5]Tromp, J. C., and Beran, P. S., "Temporal Evolution of Three-Dimensional Vortex Breakdown from Steady, Axisymmetric Solutions," AIAA Paper 95-2310, June 1995.

[6]Lele, S. K., "Compact Finite Difference Schemes with Spectral-Like Resolution," *Journal of Computational Physics*, Vol. 103, Nov. 1992, pp. 16–42.

[7]Faler, J. H., and Leibovich, S., "Disrupted States of Vortex Flow and Vortex Breakdown," *Physics of Fluids*, Vol. 20, No. 9, 1977, pp. 1385–1400.

[8]Seydel, R., *From Equilibrium to Chaos: Practical Bifurcation and Stability Analysis*, Elsevier, New York, 1988.

[9]Brown, G., and Lopez, J., "Axisymmetric Vortex Breakdown, Part 2: Physical Mechanisms," *Journal of Fluid Mechanics*, Vol. 221, Dec. 1990, pp. 553–576.

[10]Darmofal, D. L., "The Role of Vorticity Dynamics in Vortex Breakdown," AIAA Paper 93-3036, July 1993.

Finite Element Analysis of Laminated Composites Using an Unmixing–Mixing Viscoplastic Model

Seung-Jo Kim* and Eui-Sup Shin†
Seoul National University,
Seoul 151-742, Republic of Korea

Introduction

ADVANCED composites in high-temperature environments, e.g., various aerospace applications, exhibit inelastic behavior such as creep and plasticity interaction. For example, thermoplastic composites have improved fracture and damage tolerance properties owing to the increased matrix ductility. Also, metal matrix composites show an appreciable viscoplastic deformation in severe thermal conditions. Therefore, characterizing the viscoplasticity is indispensable for reliable analysis and design of composite structures in such environments.

However, the intrinsic nonlinearity of viscoplastic phenomena and the anisotropy of composite materials increase difficulties in analyzing the viscoplastic behaviors. Many kinds of constitutive models were proposed to simulate the rate-dependent plasticity of composite materials. Most of them were modified or/and extended from classical or the unified viscoplastic models of isotropic materials.[1–3] However, these macroscopic theories fundamentally have some disadvantages in identifying the constitutive relations. Mainly, it is difficult and self-empirical to determine the appropriate form of anisotropic functions (or functionals) with vector and tensor invariants required in a yield criterion, flow potential, dissipation energy potential, etc. From a practical viewpoint, evaluating various material constants used in the macroscopic equations is very expensive and time-consuming.

Received Oct. 31, 1994; revision received Oct. 10, 1995; accepted for publication Oct. 30, 1995.

*Professor, Department of Aerospace Engineering. Member AIAA.
†Graduate Research Assistant. Member AIAA.